J. Fluid Mech. (1999), *vol.* 390, *pp.* 297–323. Printed in the United Kingdom

The flickering candle: transition to a global oscillation in a thermal plume

By T. MAXWORTHY

Department of Aerospace and Mechanical Engineering, University of Southern California, Los Angeles, CA 90089-1191, USA and PMMH-ESPCI, 10, Rue Vauquelin, Paris 05, France

(Received 19 November 1997 and in revised form 1 February 1999)

A number of experiments have been performed on the properties of propane diffusion flames at relatively low fuel flow rates and using a variety of burner types. Optical methods were used to observe the flame and plume above it. We have studied the transition from a steady flame, with a plume exhibiting a helical instability at low flow rates, to an axisymmetric instability of the whole flame/plume, that grows from the base of the flame and oscillates at a well-defined and robust frequency, at higher flow rates. These results and the observation of the effects of various external modifications, e.g. the generation of an annular counterflow, a pressure perturbation, etc. are consistent with the view that the transition to the axisymmetric state, at which the flame flickers, is one to a globally excited oscillation forced by a region of absolutely unstable flow at or near the base of the burners used in this study.

1. Introduction

Observations of flickering, i.e. oscillating, diffusion flames have certainly been made since the discovery of fire and the subsequent use of a animal fat or vegetable oil, and some form of wick, for lighting purposes. Over the millennia the techniques for the control of the oscillation have evolved on a trial-and-error basis. In particular various forms of surrounding 'chimney' have been designed that enabled the use of a bright, long, steady flame that would have flickered at a psychologically disturbing frequency without its use. In this case the co-axial flow induced in the chimney by the flame's convective plume is certainly the stabilizing agent. In fact it has been found that quite subtle changes in the flame's environment can change the fuel flow rate at which flickering starts.

The 'modern' study of the phenomenon probably began with the work of Lord Rayleigh, and others referenced in Rayleigh (1929), who used flames as amplifiers of sound in resonance tubes or cavities. In this case the sound intensity was usually of sufficient magnitude to force the flame to oscillate and release heat periodically at the resonance frequency of the tube or cavity. More recently the phenomenon has been the source of a large number of experimental studies; see, for example, the bibliographies in Hamins, Yang & Kashiwagi (1992); Lingens *et al.* (1996*a*, *b*); Zukoski, Cetegen & Kubota (1984); etc. In general, for a given burner and fuel type, oscillation has been reported to begin at a certain flow rate. (See, however, the present results where the transition has been found to take place over a small range of flow rates.) Oscillation frequencies have been measured in the approximate range of 0.5 Hz, for the largest diameter pool fires (25 m) (Schoenbuecher *et al.* 1986) to 16 Hz for the smallest (0.5 cm) gas jets with the largest jet velocities ($3\,\mathrm{m\,s^{-1}}$) (Hamins *et al.* 1992). The

phenomenon has been associated with the instability of the heated jet flow or plume generated by the flame and with the subsequent rapid formation of large-scale vortices which, upon interaction with the flame itself, cause a visible fluctuation in the flame height (Chen & Roquemore 1986; Chen *et al.* 1988, 1992; Schoenbuecher *et al.* 1986; etc.). An important summary paper on the numerical computation of axisymmetric diffusion flames that exhibit the types of oscillation of interest here is that of Katta *et al.* (1996). The reference list to that paper also includes some of the papers that preceded it in which the instability of the flame-induced buoyant jet were clearly revealed. The frequency of oscillation calculated by them, 15 Hz in Katta, Goss & Roquemore (1994) for example, are within the range found experimentally (Hamins *et al.* 1992) for the 1 cm diameter jets they considered in that study. Unfortunately, these authors did not discuss the source of the oscillations in terms of convective/absolute instability and global modes as considered here.

With these observations, and others, as a source of information a number of theoretical studies have been undertaken (Buckmaster & Peters 1986; Yuan 1993; Yuan, Durox & Villermaux (1994); Durox, Yuan & Villermaux 1997) in which classical stability theory has been used. That is the flow has been assumed to be locally parallel and the convective instability of that flow calculated. In this case one finds that the local instability frequency depends on the height above the burner in the spatially evolving experimental or theoretical mean flow. Yuan *et al.* (1994) chose a value for the local Reynolds number of 150 at which instability was assumed to occur, while Buckmaster & Peters (1986) simply chose a height of 3 cm for the case they considered. Both gave values of frequency close to those observed. However, our present observations and others show that the oscillation often starts at the lip of the burner itself, i.e. the instability height is zero, or, at least, this height is considerably smaller than that calculated by assuming the relatively large value of the Reynolds number given above! In what follows we take an alternative point of view.

Many of the observations to date, and those presented in the main body of this paper, are consistent with the assumption that there is a finite axial region of absolutely unstable flow with the consequent self-excitation of a global mode (Huerre & Monkewitz 1990, referred to as HM in what follows). In this case even though the local absolute instability frequency may vary spatially the system 'chooses' a frequency based on the overall characteristics of the absolutely unstable region. A number of possible ways of choosing this frequency are given in HM with the most likely being "the value found at the saddle point of the local absolute frequency in the complex plane of the 'slow' spatial scale"; see their equation (40). The criteria introduced by Koch (1985) and Pierrehumbert (1984) are different from the one given above. The latter, in a study of baroclinic instability, used the real part of the complex frequency at the streamwise location of maximum absolute growth rate. The former used the value of the frequency calculated at the boundary between the convective and absolute regimes. It is perhaps here that one can see a possible connection between the convective stability calculations of Buckmaster & Peters (1986) and the absolute stability point of view taken here. Since Buckmaster & Peters (1986) need an axial location at which to calculate a frequency Koch's (1985) criterion can give it. Koch's (1985) criterion was also used by Lingens *et al.* (1996*a*, *b*), in a study closely related to the present one, in which they studied a high-speed jet diffusion flame. In fact, this latter study is the only one known to us that applies such 'global-mode' ideas to the oscillation of diffusion flames. In their measurements the jet speed was so large that the lower 10 mm of the flow from a 10 mm nozzle was convectively unstable to become absolutely above this location, in one reported case.

Alternative mechanisms are also known to excite global oscillations. For example the generation of 'edge tones' is known to be caused by the feedback, to their origin, of pressure perturbations from unstable shear-layer vortices impinging on a solid surface. In what follows we show how, in the present case, this effect can modify the criterion for the onset of the oscillations that normally occur in its absence.

In what follows we study this system from a slightly different point of view from that of Lingens *et al.* (1996*a*, *b*), for example we observe the transition to a global oscillation as the fuel flow rate is varied from a small value, at which the flame does not oscillate, to a value at which it does. By observing and measuring the plume above the visible flame we are able to observe the details of the transition from one form to the other and make measurements that suggest that a global mode is, in fact, excited.

One model that is useful in characterizing the absolute/convective nature of these flows is that found in HM (pp. 505–506), in which wake/jet flows are approximated by a parallel variable-density vortex-sheet example, but with no buoyancy effects included. Here, and in a number of experimental observations given in the same review, it is clearly shown that jet flows, of the type of interest here, undergo a convective-to-absolute transition if a counterflow is superimposed. This is also true if the jet is heated to a sufficiently high temperature. In both cases the most unstable oscillation has a 'varicose' or axisymmetric mode shape. Of course, this does not mean that the regions of absolute instability are large enough to support a global mode but they are suggestive that such a state is attainable. In contrast it can be shown that an absolutely unstable flow can be stabilized, and the flow undergoes a transition to a convective instability, if a coflow is superimposed, as in the case of the flow induced by a chimney in the present case.

2. Apparatus and experimental methods

The basic flow apparatus is shown in figure 1. It consisted of a number of burners, the characteristics of which are considered later, mounted within a surrounding tube, of 2 in. (5.08 cm) diameter, within which a counterflow could be generated. An extension tube could be installed to increase the height of the tube by 1 in. (2.54 cm). Both tube and extension could be removed so that the burners could operate in 'free air'. The whole burner assembly was placed inside a plastic tank that was 30×30 cm in cross-section and 60 cm high. This tank had a number of 1 in. (2.54 cm) holes drilled near its lower end to allow the entry of relatively undisturbed room air. After a large number of trials, the unsteady recirculation of air from the surroundings was prevented by placing an aluminium sheet over the exit to the tank and drilling a 5 cm diameter hole at its centre. In this way a region of stratified air, plus combustion products, was formed at the top of the tank. This prevented ambient air from entering the top of the tank but allowed the heated air to exit at an appropriate rate.

A number of burner types were used in order to cover as wide a range of conditions as possible, all of which are sketched in figure 2. Four were of 'conventional' type, i.e. they consisted of straight brass tubes of diameters $\frac{1}{8}$, $\frac{1}{4}$, $\frac{1}{2}$ and $\frac{3}{4}$ in. connected, through a turbulence-reducing screen, to a bank of flowmeters of the 'rotameter' type. These burners are similar to those used in previous studies, e.g. Hamins *et al.* (1992), and were used to compare with the results of those studies. In what follows they are called 'straight' burners as a short-hand identification. The second group of burners were of a type that did not introduce axial flow momentum directly into the flow field, as did the ones discussed above. These were thought to act more like true candles

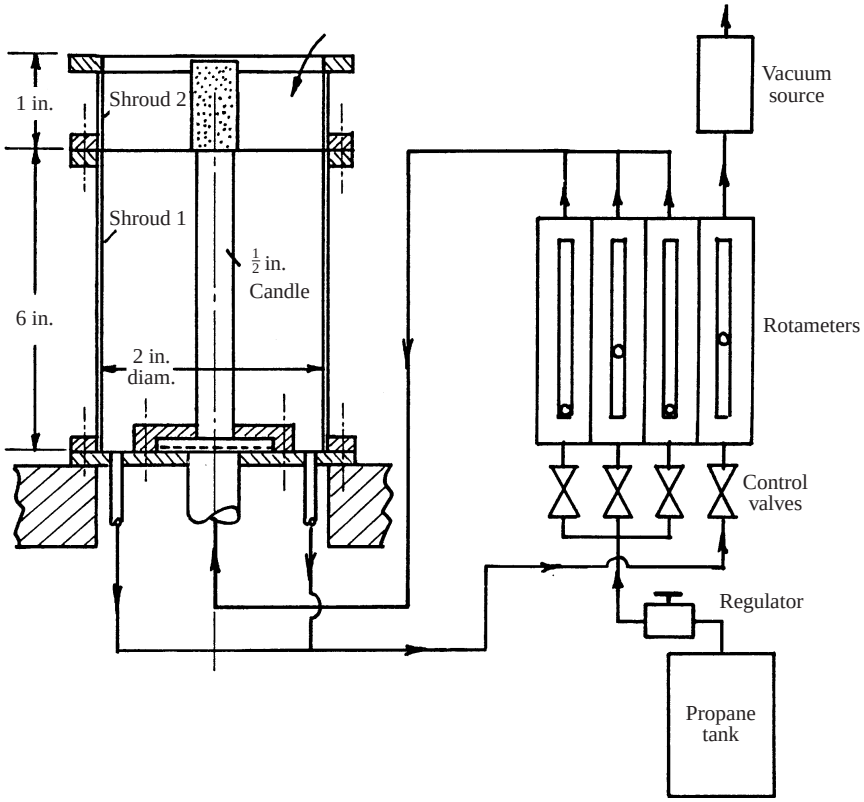

FIGURE 1. Flow apparatus showing the $\frac{1}{2}$ in. candle in place surrounded by the two 2 in. shrouds.

without the obvious disadvantages of the latter. The first was an $\frac{1}{8}$ in. diameter tube, closed at the upper end, with eight 1 mm holes drilled at that end. Thus the outflow of fuel was radial and axial momentum could be produced only by the buoyancy of the combustion products and entrained ambient air. The second was a $\frac{1}{2}$ in. diameter by 1 in. long fritted glass cylinder, mounted on a glass tube, that was porous to the gas flow, and had characteristics similar to those of the smaller burner. This latter burner could be fitted with an extension tube that was used to determine the effect of possible flow separation at the top of the basic burner (see figure 2). Both of these are called 'candle' burners or 'candles' in what follows. In all cases the fuel used was reagent grade propane.

The instrumentation used to study these flows was of two types in the absence of any way of measuring the flow velocity, e.g. LDV or PIV. The first, and simplest, was a shadowgraph system using a standard slide projector. A standard slide with a 4 mm diameter hole cut at its centre was used to reduce the source size to a useable magnitude. An image of the thermal plume from the flame was projected onto a white sheet and video taped at 25 f.p.s., with an exposure time between 1/500th and 1/1000th of a second.

The second instrument was a CCD camera with a single linear array of 2056 pixels that had a frequency response to 2000 Hz. This device could only be used to study the time response of the luminous flame, and was especially useful in determining its frequency and amplitude variations with time. Typically a scanning frequency of

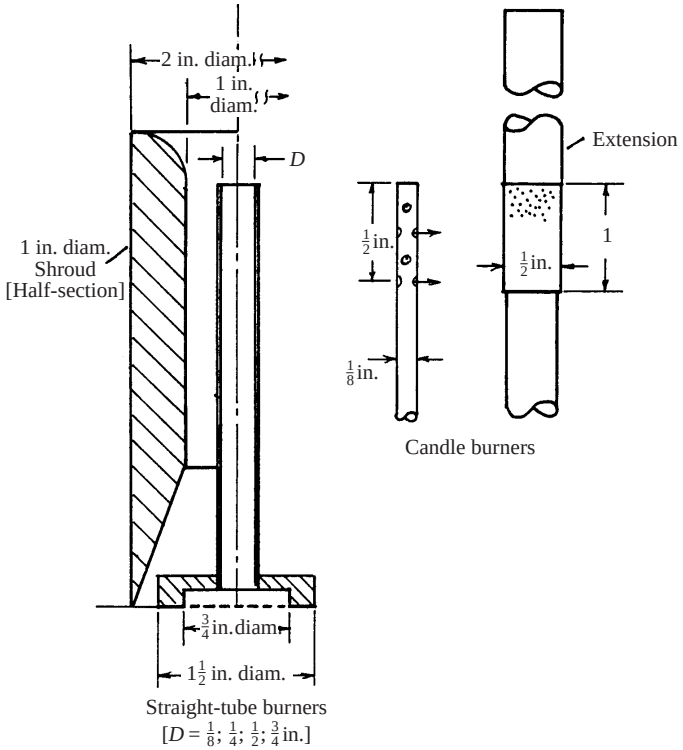

FIGURE 2. Details of the burner types used in this study.

200 f.p.s., and a run duration of 10 s, was used to give a total of 2000 points, at 20 points/cycle for a flame frequency of order 10 Hz. Also, only approximately 200–250 pixels were used to cover the total flame height, or width. In this way computer storage requirements were kept to a minimum. Despite these restrictions over 55 Mbytes of data were taken and stored as MS Excel files.

In order to fully study the system response a number of preliminary tests were run with each of the burner types. It quickly became clear that the amount of data that was likely to result from an exhaustive program with all of them would be overwhelming, and reporting everything would mask the simple message we wished to present. Therefore we finally settled on a study with burners that gave the most unambiguous results, i.e. the two candle burners and the $\frac{1}{8}$ in. straight burner. The others are used only sparingly in order to illustrate a particular point. For the chosen burners their natural, i.e. unforced, characteristics were first found followed by their response to pulsed forcing and various forms of external flow.

3. Results

Results of the tests carried out on the series of burners discussed above are difficult to organize since a great deal of information has been gathered. Usually we present data on a particular characteristic for all the burners at the same time, unless a special point has to be emphasized.

3.1. *Intermittency of, and critical flow rate needed to attain, the flickering state*

As the flow rate was varied for any particular burner it was found that the flickering state did not suddenly appear at one special value. At low flow rates the flame was stable but the plume above the flame was unstable to *helical* disturbances, as in the first few frames of figure 3. This instability appears to be of mode type $m = \pm 1$. It is not possible to distinguish between them using the present experimental scheme. A small increase in flow rate caused a partial transition to the flickering state, i.e. the appearance of flickering was intermittent. A sequence of ordered video images of this transition is shown in figure 3 for the $\frac{1}{8}$ in. candle (since the flicker frequency was close to one half of the video aquisition rate it was necessary to reconstruct this sequence from many cycles of the oscillation). One can see that the helical instability approaches the flame, the tip of which is marked on the first frame, and becomes *axisymmetric*, with wavenumber $2\pi d/\lambda \approx 1.8 \pm 0.2$, where d is the plume diameter and λ the wavelength of the instability. In frame (h) this symmetric disturbance is interacting with the flame causing it to oscillate. The growth, and later decay, of this oscillation was also captured by the linear camera and usually it was approximately exponential in time. In figure 4 a 10 s sequence of the oscillation is shown for the $\frac{1}{8}$ in. candle and a flow rate of 29.4 ml min^{-1}. The growth and decay of the first packet in this sequence are shown in figure 5, where the straight lines represent an exponential time behaviour. The low-level oscillation between the two packets is not discernible by the naked eye and the corresponding video images show a helical disturbance above the flame. The frequency measured form this sequence is 11.2 ± 0.2 Hz and thus is essentially the same for the helical and axisymmetric modes. There is some suggestion in video sequences taken far downstream that the axisymmetric state reverts to a turbulent helical mode but to prove this would require more sophisticated instrumentation than used here.

Four minute video sequences were taken of the shadowgraph image for several of the burners and at a number of flow rates. These were then reviewed and an estimate made of the percentage of time the flow was in the flickering state, i.e. when the whole plume was oscillating in the axisymmetric mode. Figure 6 shows a plot of this intermittency function versus flow rate for four cases. The two central curves are for the $\frac{1}{8}$ in. and $\frac{1}{2}$ in. candles in free air. They are essentially indistinguishable to within experimental uncertainty. The two outer curves show how these basic results are affected by the introduction of small changes to these conditions. In the first, the rightmost curve, a $\frac{1}{2}$ in. extension was added to the $\frac{1}{2}$ in. candle in order to remove the likely stagnation region behind the burner. In this way one could remove any suspicion that the oscillation was caused primarily by the instability of the wake flow above the burner. Figure 7 presents an ordered sequence of video images of this case for a relatively large flow rate (33.7 ml min^{-1}). The formation of intense vortices in the accelerating outer shear layer of the plume can be seen clearly. These are to be compared with the flow visualized in the cases shown in figure 8 of the $\frac{1}{2}$ in. candle operating alone at two different flow rates: 31.3 and 42.9 ml min^{-1}. Here we see that vortex formation is less intense than with the central extension tube in place and that, at the lower flow rate, the far plume tends towards a spiral state even as the near plume vortices are axisymmetric. Also of critical importance is the observation that, in this case, the axial extent of the flame or heat source is small (it is shown dotted in the images of figure 8). This is turn implies, but does not prove, that the details of the flame structure are likely to be important in determining the stability of the flow and that it simply acts as a heat source.

Finally the leftmost curve of figure 6 shows the effect of introducing an obstacle downstream of the $\frac{1}{8}$ in. candle. A sequence of images is to be found in figures 9 and

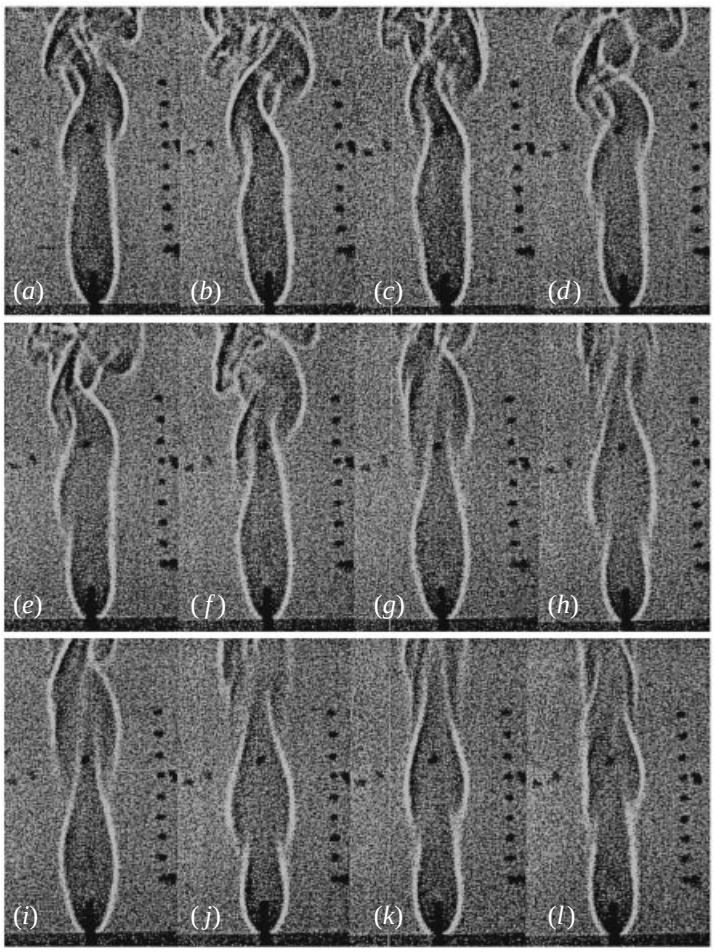

FIGURE 3. Time series showing transition from a helical disturbance to an axisymmetric one in the intermittent regime for the $\frac{1}{8}$ in. candle. The horizontal line in the first frame indicates the height of the undisturbed flame tip.

10 for the cases where the base of the obstacle is 3.9 cm and 2.1 cm downstream of the top of the burner, respectively. Here the aim was to show that the interaction of the plume with the obstacle increased the sensitivity of the plume to disturbances, i.e. a given intermittency occurred at a lower flow rate with the obstacle present. Here, the flame tip was 1.5 cm below the obstacle, at a flow rate of 25.7 ml s^{-1}, in figure 9(*a*) and at the obstacle base, at a flow rate of 30.6 ml s^{-1}, in figure 9(*b*). One might interpret this result as showing that the feedback of pressure disturbances generated by interaction of the plume and obstacle positively reinforced the original disturbance. This then gives an increased response *vis-à-vis* the undisturbed case. In figure 9(*a*) the two basic forms of oscillation are shown. In the left-hand image oscillation began at the location of the obstacle, i.e. the plume below the obstacle did not oscillate, and the instability amplitude was small. In the right-hand image the whole plume was oscillating, i.e. the oscillation amplitude began to grow at the lowest point of the flame/plume (see § 3.3). In figure 10, at a flow rate of 34.3 ml s^{-1}, we show the flickering state when the candle–obstacle distance was reduced. Here and in

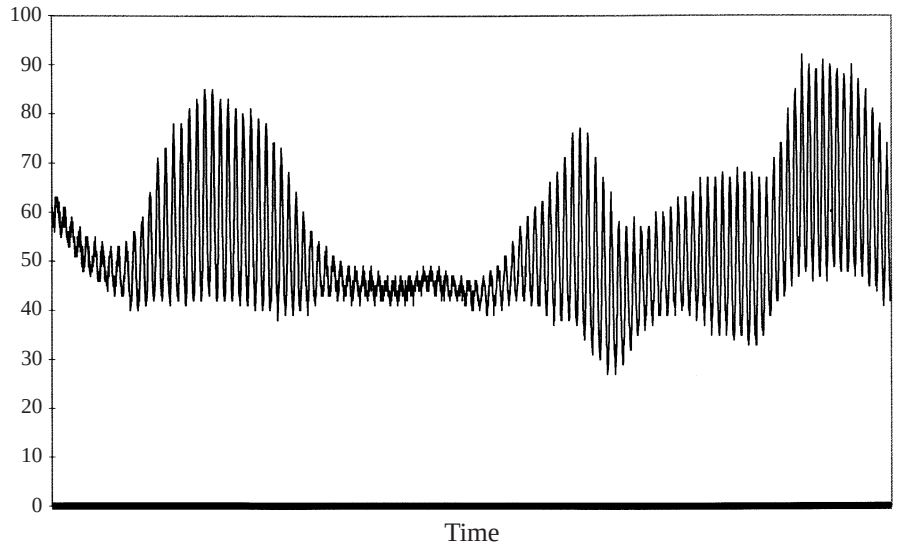

FIGURE 4. Natural response of the $\frac{1}{8}$ in. candle at a flow rate of 29.4 ml min^{-1}. The intermittency of the flickering oscillation is clearly shown. Here and in all similar figure the total time span of the abscissae is 10 s.

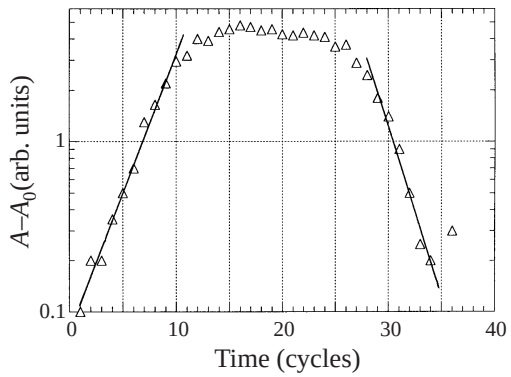

FIGURE 5. Flame amplitude versus time in cycles for the case shown in figure 4.

figure 9 the frequency of oscillation was reduced over the unobstructed case but the intervortex spacing was smaller, indicating a reduction in the convection velocity of the vortices in this case. Further comments on these and similar results are postponed until § 3.2.

These types of measurement were repeated using the straight-tube burners. In figure 11 we show a measure of the critical flow rate (Q_c), i.e. the rate at which the intermittency was approximately 50%, versus tube diameter. Upon reinterpreting the results of Hamins *et al.* (1992) in terms of flow rate, one finds reasonably good agreement between the two sets of measurements. In the present work we find that

$$Q_c = 77.1\mathrm{D}^{0.57},$$

while Hamins *et al.* (1992) obtained:

$$Q_c = 90.5\mathrm{D}^{0.59}.$$

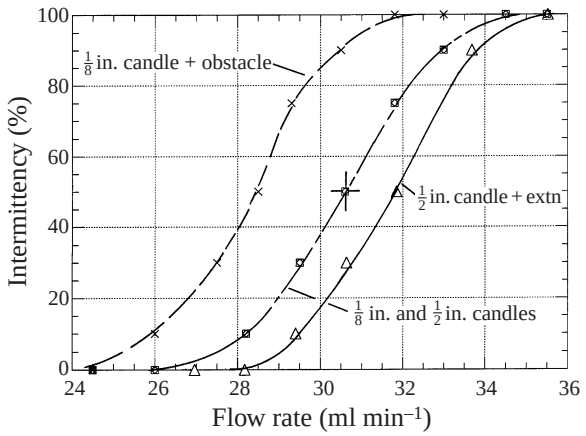

FIGURE 6. Intermittency versus flow rate for four burner configurations.

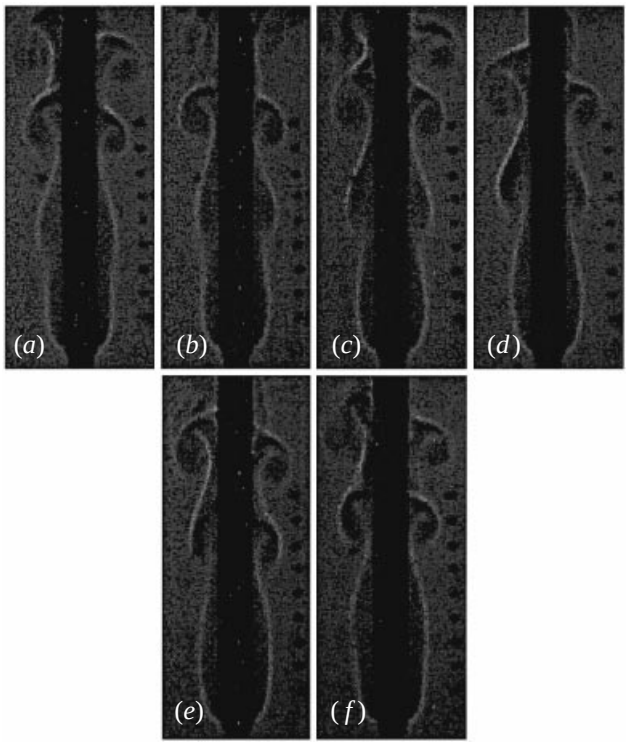

FIGURE 7. Time series showing the growth of axisymmetric disturbances over an extension to the $\frac{1}{2}$ in. candle burner at a flow rate of 27.5 ml min^{-1}.

where Q_c is in ml min^{-1}, and D in cm. One assumes that the 15% difference between the constants of proportionality is probably due to a slightly different definition of the critical flow rate in the two cases and to different designs for the burner and its enclosure. Also note that the critical flow rate for the $\frac{1}{8}$ in. straight-tube burner is less than that for the equivalent $\frac{1}{8}$ in. candle (figure 6). This indicates that the jet momentum, in the former case, enhances the axial, buoyancy-driven flow sufficiently to require less heat input to arrive at a similar, unstable state.

(*a*)

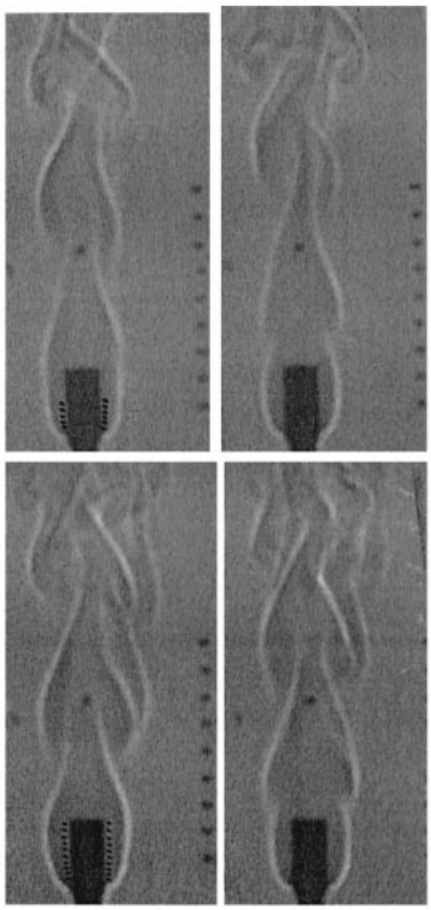

(*b*)

FIGURE 8. Generation of axisymmetric waves/vortices for the $\frac{1}{2}$ in. candle burner and (*a*) a flow rate of 31.3 ml min^{-1} and (*b*) 42.9 ml min^{-1}. The lengths of the visible flame are shown dotted in each case. From these examples it is clear that the instability is mainly one of the plume generated by the flame rather than of the flame itself, in this case.

3.2. *The frequency of oscillation*

The frequency of oscillation was measured for several burner/flow rate combinations using the linear camera. A typical result is shown in figure 12 for the case of the $\frac{1}{8}$ in. candle at 42.9 ml min^{-1}, i.e. well into the continuously oscillating regime. The measured frequency is 11.1 ± 0.15 Hz, i.e. it is constant to approximately $\pm 1.5\%$ over this 10 s period and is the same at all heights within the visible flame. In response to a query by a referee we note that this frequency was the same at all axial locations in the flame, again a response typical of a globally exited oscillation. Such a stable oscillation is very typical of feedback oscillators, in this case a global mode (see e.g. HM), and is one of the reasons we thought, initially, to try to strengthen the evidence for such an identification. As has been shown a number of times before, this frequency is insensitive to changes in flow rate, as shown for this case in figure 13. The first point, which is in the regime where the intermittency is close to

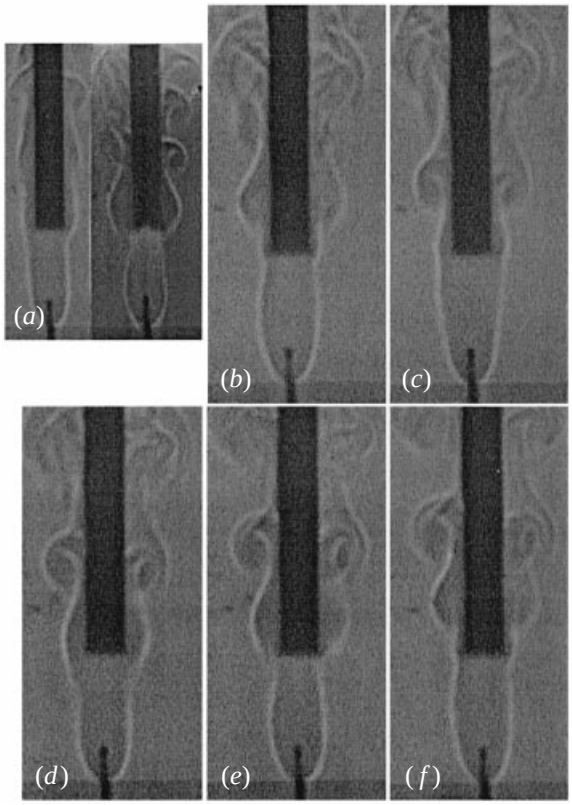

(*b*)

FIGURE 9. Time series showing the effect of an obstacle 3.9 cm above the burner on the stability of a plume from the $\frac{1}{8}$ in. candle. (*a*) In the intermittent regime for a flow rate of 25.7 ml min^{-1}. The first image shows the case where the oscillation begins at the obstacle; the second when the whole flame/plume is oscillating. (*b–f*) Flow rate 30.6 ml min^{-1}. The whole heated column oscillates at all times.

zero, was taken from the response of the flame to an external pressure pulse that generated a train of regular oscillations that decayed slowly in amplitude. For this reason this result may be atypical, but seems to follow the general trend of the data in a reasonable way. Similarly the $\frac{1}{2}$ in. candle produced a 10 ± 0.1 Hz oscillation for flow rates between 40 and 65 ml min^{-1}.

In figure 14 we show the essentially constant frequency of oscillation, over the small range of low flow rates covered, versus tube diameter, for the straight-tube burners (typical uncertainty is ± 0.5 Hz, i.e. somewhat larger than that found for the candle burners). Also plotted are two of the results of Hamins *et al.* (1992) for their lowest flow rates and that overlap our values of diameter, where the frequency was also constant. The data agree well except for the somewhat high value for the $\frac{3}{4}$ in. (1.9 cm) burner. The reason for this anomaly is not clear at the moment.

As noted previously the insertion of an obstacle or the addition of an extension had a large effect on both the critical flow rate and the frequency of the resultant oscillation. Thus the insertion of a 1.6 cm diameter rod into the plume from the $\frac{1}{8}$ in. candle (figures 9 and 10) reduced the frequency to approximately 6.0 ± 0.5 Hz for burner to obstacle spacings of 3.9 cm and 5.4 cm, and to 8.0 ± 0.5 Hz for a spacing of

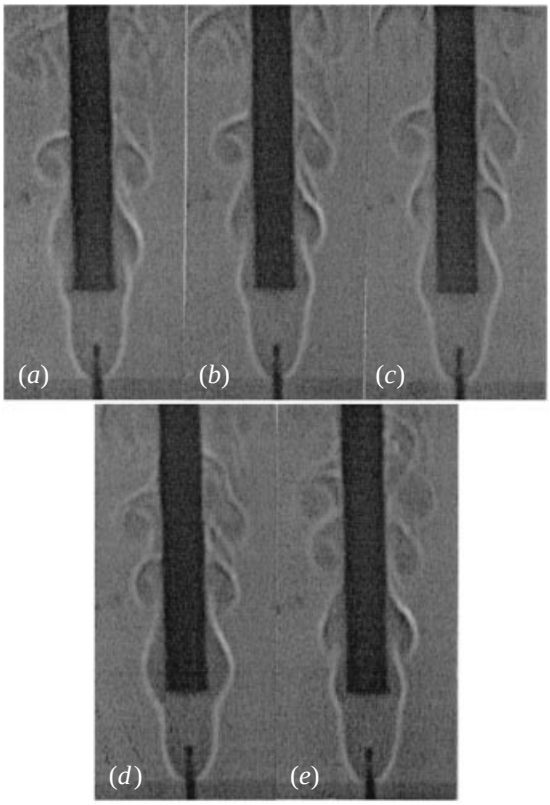

FIGURE 10. As in figure 9 but for a obstacle to burner spacing of 2.1 cm and a flow rate of 34.3 ml min^{-1}.

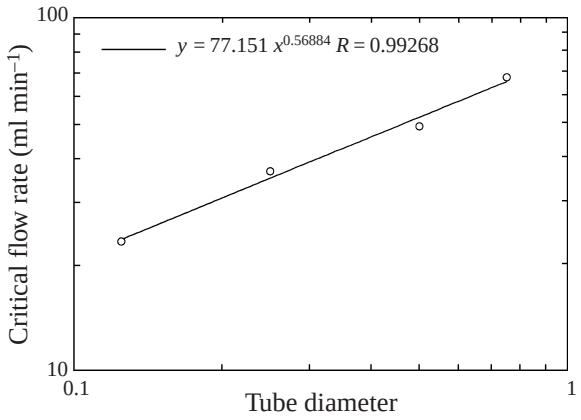

FIGURE 11. Critical flow rate versus tube diameter for the straight tube burners.

2.1 cm. At the same time the wavelength between the vortex structures was reduced. For example, the distance between the first vortex pair of figure 10 is approximately 3.0 ± 0.5 cm, and this is more generally true for other burner–obstacle spacings, while the vortex spacing for the undisturbed $\frac{1}{8}$ in. candle plume is 5.5 ± 0.5 cm (figure 15). Thus the vortex convection velocity, which is presumably of the order of one half

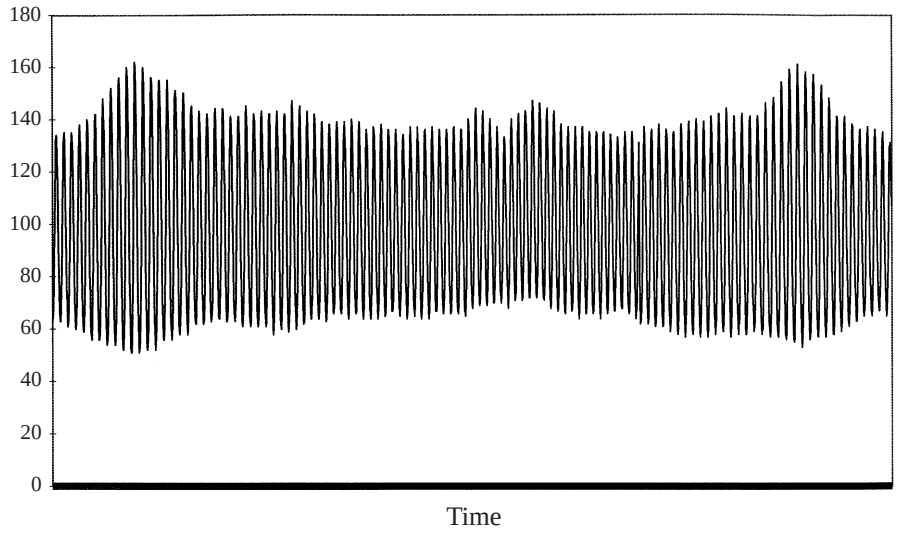

FIGURE 12. Amplitude versus time or natural oscillations at a flow rate of 42.9 ml min^{-1}, i.e. beyond the intermittent regime.

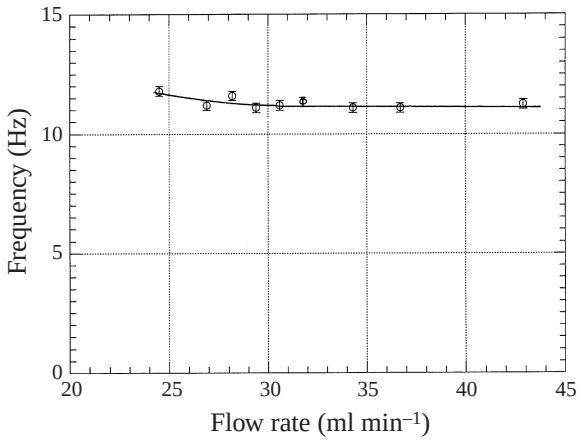

FIGURE 13. Frequency of oscillations versus flow rate for the $\frac{1}{8}$ in. candle burner.

of the maximum plume velocity, is $18 \pm 3\,\mathrm{cm\,s^{-1}}$ in the first case and $61 \pm 6\,\mathrm{cm\,s^{-1}}$ in the second. This suggests, not surprisingly, that the flow over the obstacle greatly reduced the plume velocity, in this case by a factor of more than three. Note that the maximum velocity estimate for the free flame, i.e. $122 \pm 12\,\mathrm{cm\,s^{-1}}$, is virtually the same as that measured by Lingens *et al.* (1996*a*, *b*) at a height of 10 cm above the flame, when one excludes the high-speed central velocity peak generated by their large jet velocity ($140\,\mathrm{cm\,s^{-1}}$). This is the velocity estimated at essentially the same height in the present case.

3.3. *Growth of the instability amplitude*

As can be seen clearly in all of the video sequences the amplitude of the oscillations grew with distance downstream. From the point of view taken here there is a distinctive difference between the behavior of convectively and globally unstable

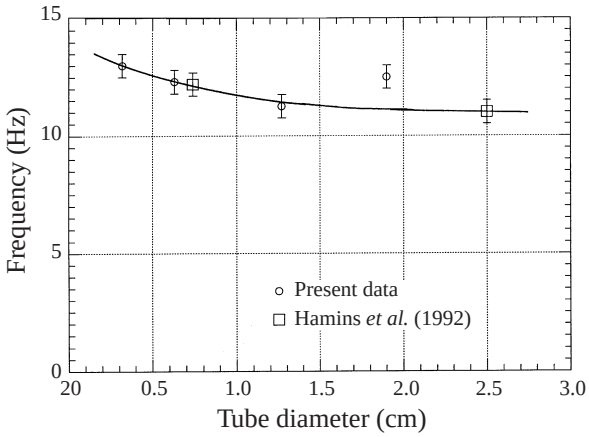

FIGURE 14. Frequency versus tube diameter for the straight tube burners. Also shown are the data of Hamins *et al.* (1992).

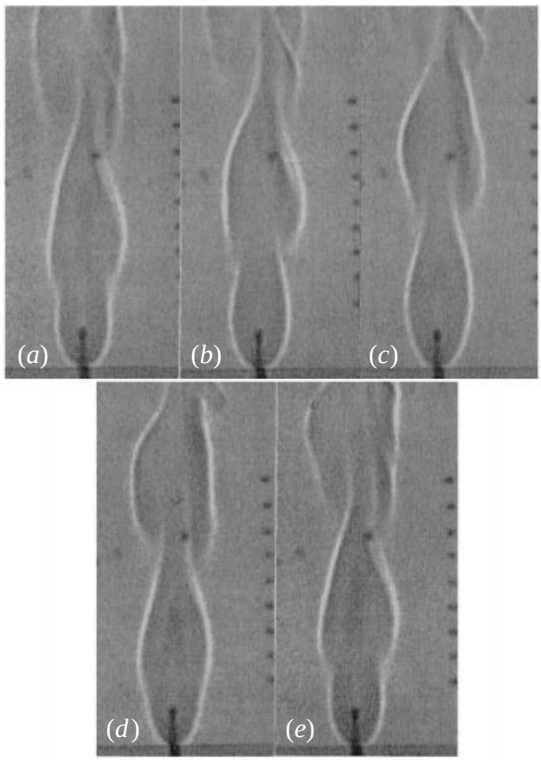

FIGURE 15. Time series showing the oscillation of the flame/plume for the $\frac{1}{8}$ in. candle at a flow rate of 42.9 ml min^{-1}. The dots at the rightmost margin are 1 cm apart.

flows. In the first case, as shown theoretically by Buckmaster & Peters (1986) and in a series of papers by Durox, Yuan & Villermaux, e.g (1997), in a spatially evolving flow the calculated frequency of oscillation depends strongly upon axial location. Thus the first authors' simply chose a value of 3 cm, while the second assumed

that instability began when the local Reynolds number, based on the maximum convective velocity, shear layer thickness and plume viscosity, reached a value of 150. Thus the convective instability point of view requires that the instability start at a finite distance from the thermal source. On the other hand globally unstable flows are excited by the whole region of absolutely unstable velocity and temperature profiles, which then acts as a source of forcing. In this case one frequency is chosen based on the global properties of the evolving flow. In the present case, as in the related problem of the dripping faucet (see HM, p. 516, for example), the region of absolute instability starts at or near the base of the flame and, when it grows to sufficient length, a global response is generated. Thus one would expect in this case that the oscillations would start growing close to or at the source not several centimetres downstream.

In order to demonstrate this possibility three results are presented here. First, and most simply, one can compare the shapes of the plume at two times one half-period apart. This result is shown in figure 16 for the $\frac{1}{8}$ in. candle flame at a flow rate of $36.7\,\mathrm{ml\,min^{-1}}$. One is an original image and the dotted curves show the shape traced from an image taken one half-period later. One can see clearly that the flame motion starts at the base of the flame and grows in amplitude further downstream. A similar demonstration makes use of the image processing program used, NIH Image, which allows one to average a number of video images, in this case one hundred. The result is shown in figure 17 for the cases of the $\frac{1}{2}$ in. candle. On the image we have drawn curves representing the extremes of the plume excursions. Again it is evident that the oscillation starts at the base of the flame and grows rapidly to virtually saturate only 7–10 cm above the burner. Finally NIH Image can be used in its 'spatio' mode. That is a line of pixels can be chosen on the video image and a space–time moving picture made of that line. By repeating this process at several axial locations, and then measuring from the space–time history of the plume excursion, one can construct the graph shown on figure 18, in this case for the $\frac{1}{2}$ in. candle plus extension. One notes almost exponential growth initially followed by a great reduction in growth rate approximately 5 cm downstream and an approach to saturation. Of course further downstream than measured here the vortical flow structures break down to form a turbulent plume, the dynamics of which are different from those of interest here since growth is now by three-dimensional, turbulent processes.

However all three types of measurement indicate growth from the very beginning of the thermal field, and strongly favour the global response hypothesis being tested here.

3.4. *Response to external disturbances*

3.4.1. *Response to rapid changes in flow rate*

In this sequence of tests the fuel flow rate was suddenly increased from a value at which oscillations never occurred to one at which they did. After a number of cycles the flow rate was suddenly reduced to its former value. We estimate that the rate changes took place within 1/10th of a second. The time response of the oscillations was detected by the linear camera by measuring the sequence of adjacent peak-to-trough amplitudes for each cycle and plotting as a function of the cycle number. Two typical results are shown in figure 19. In both cases growth to the final amplitude takes place within 3 or 4 cycles, while the apparent exponential growth and decay may be fortuitous, since so few points are available to define them.

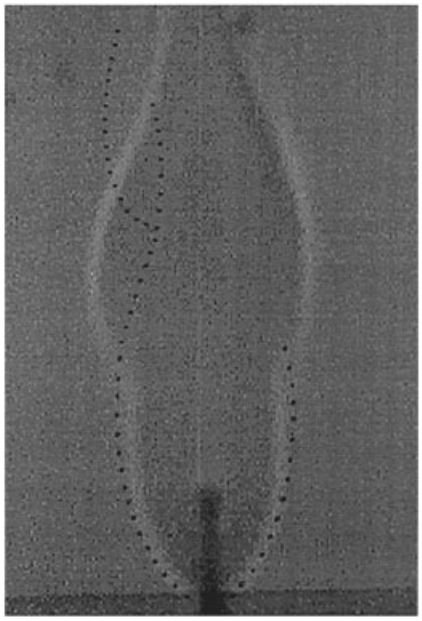

FIGURE 16. Superimposed views of the plume from the $\frac{1}{8}$in. candle. The images were taken $\frac{1}{2}$ period apart and show that the oscillation starts at the flame base. Flow rate 36.7 ml min^{-1}.

3.4.2. *Response to a counterflow*

In many ways this is the most interesting and complex result from this work. We present results using the $\frac{1}{8}$ in. straight tube burner mounted inside the two shrouds shown in figure 1. A counterflow of 2.5 cm s^{-1} was suddenly applied to flames burning at a low flow rate (14.4 ml s^{-1}), i.e. below the flickering state. Here the model of HM is useful in anticipating the likely outcome. Their results would suggest that a backflow could cause a transition to an absolutely unstable state at which oscillation could occur if the region of absolute instability were large enough. In the present case the response was more complex but agreed with this description in the broadest sense. In most cases, as shown in figure 20, for example, the flame began to oscillate in the axisymmetric mode with a slowly increasing amplitude and at a relatively low frequency, 10.4 Hz in figure 20. However after a few seconds the flame developed a motion that can best be described as a precession around the central axis. This resulted in a low-frequency, helical motion of the plume on which was superimposed a weak pulsation of the flame length. A sequence of this helical motion is shown in figure 21 while the initial growth of the axisymmetric flame response in shown in figure 22. The frequency of the helical mode is 2.5 Hz in figure 21. Also, it is possible to describe the mean growth of the axisymmetric oscillation in figure 22 by an exponential function. Further comments on these results are postponed until § 4.

3.4.3. *Response to a pressure pulse*

When the flame was in its non-oscillating state it was very sensitive to external disturbances, e.g. the sudden closing of a door in a neighbouring laboratory. In an attempt to quantify this to some extent the exit to the enclosure was suddenly closed by allowing a hinged sheet of metal to drop over it. This caused a pulse at the burner exit that, in turn, caused the flame to oscillate. Three cases are presented in figures

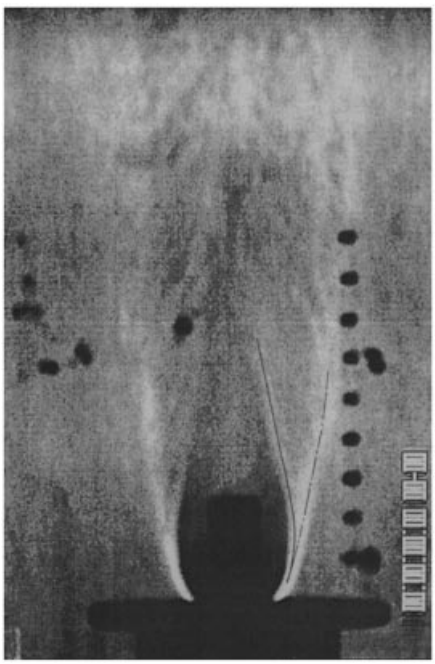

FIGURE 17. Average of 100 video images for the $\frac{1}{2}$ in. candle at a flow rate of 36.7 ml min^{-1}, showing the growth of the instability from the flame base.

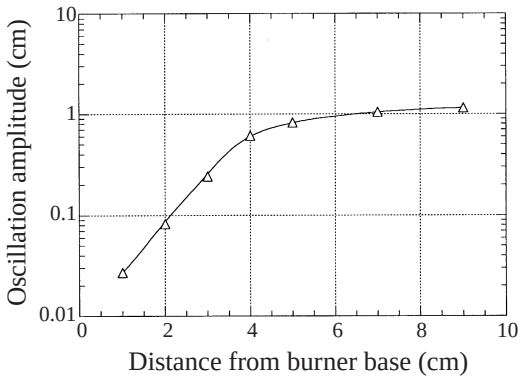

FIGURE 18. Measured oscillation amplitude versus distance from the flame base for the $\frac{1}{2}$ in. candle and extension.

23 and 24. In figures 23(*a*) and 24(*a*) the response for a flow rate of 43 ml min^{-1} is shown for the $\frac{1}{8}$ in. candle. In this case the flame is in the regime where it is always oscillating and the pulse has essentially no effect, except to increase the amplitude slightly, and decays within two oscillations, i.e. approximately 0.2 s. For flow rates of 29.4 ml s^{-1} (figures 23*b* and 24*b*) and 26.9 ml s^{-1} (figures 23*c* and 24*c*) the pulse excites an oscillation that decays over a period that is longer for the higher flow rate. Both cases are in the intermittent regime with the former having the larger value of the intermittency function. For the lower flow rate the decay starts immediately after the pulse initiates the oscillation, while for the higher there is a period, that varies from experiment to experiment, over which the amplitude is more-or-less constant for one

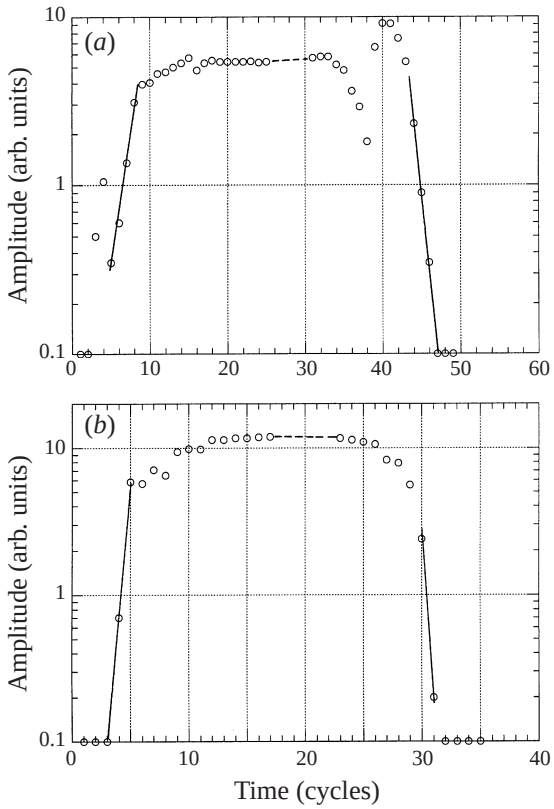

FIGURE 19. Flame response to a sudden increase and then decrease in flow rate, from 15.9 to 29.4 to 15.9 ml min^{-1}; (*b*) is a repeat of (*a*).

or two seconds. In each case an exponential curve has been drawn to represent the decay but it is usually too non-uniform for this to be more than an approximate description.

3.4.4. *Miscellaneous external effects*

In this section we report on a number of observations and measurements which we believe are important in a total description of the flow state generated by the flame. Here we present, primarily, a description of these effects with a minimum of substantiating figures, since the latter are usually more than is really needed to make a particular point.

First, the effect of the geometry of the enclosure is considered. Here, we have found that the flow state, e.g. the value of flow rate at which oscillation starts, was very sensitive to the exit details. With a smaller diameter exit hole the stratified layer in the upper part of the enclosure was deeper and oscillations began at a slightly lower flow rate. The 5 cm value chosen was the one that seemed to give the most consistent and repeatable results.

The air flow through the enclosure could be rapidly increased by placing a cylindrical chimney over the exit hole. This had the effect of increasing the effective depth of the heated layer and increasing the driving buoyancy force. An oscillating flame was stabilized by this change, as shown in figure 25 for a flow rate of 54.9 ml s^{-1} and the $\frac{1}{8}$ in. candle. Here the first image was taken immediately

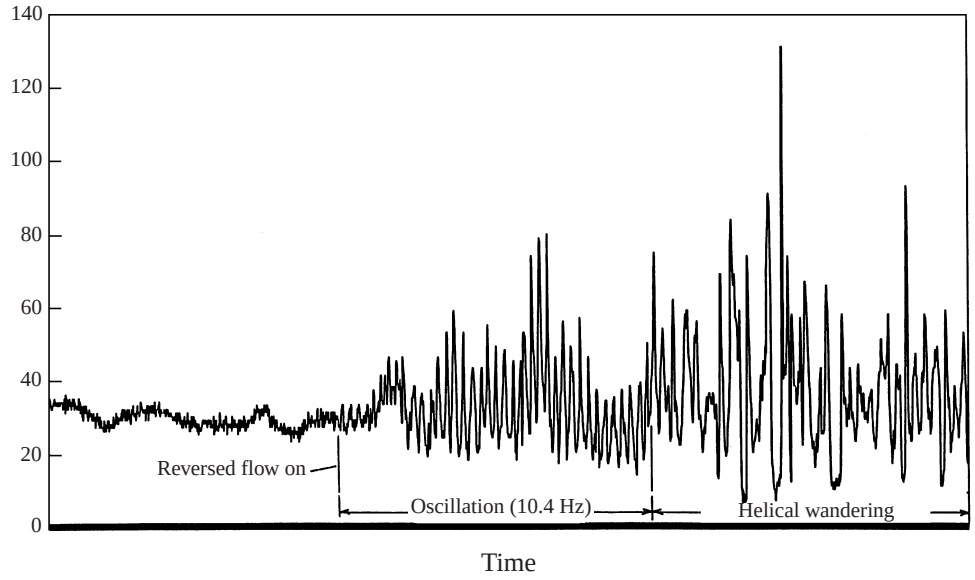

FIGURE 20. Flame response to a sudden application of a counterflow with a velocity of 2.5 cm s^{-1}, showing the slow growth of an axisymmetric oscillation followed by a transition to a helical wandering of the plume.

before the chimney was put into place, while the second was taken 15 s later and shows a stabilization of the flame and the appearance of a helical disturbance downstream. The third image was taken 15 s after the chimney was removed and one can see a return to an axisymmetric perturbation that involves the oscillation of the whole flame/plume. We assume that these changes were induced by an increase and then a decrease in the induced co-flow around the flame (see § 4).

The critical flow rate could also be changed by the presence of the shrouds around the flames. In particular changing the flow conditions at the base of the flame appears to have a large effect. When the $\frac{1}{4}$ and $\frac{1}{2}$ in. straight tube burners were placed within the main, 2 in., shroud the flame was greatly destabilized. The critical flow rate was almost halved, reduced by 54%, for the first burner and by 35% for the second. The further addition of the second, short shroud affected the critical flow rate only slightly. One can rationalize these results by assuming that the shrouds produce a counterflow at the burner base which has the same effect as the forced flow of § 3.4.2. Sketches of these are shown in figure 26(*a*). Contrariwise, simply placing the smaller shroud, alone, around and slightly above the burner lip had a very strong stabilizing effect (figure 26*b*), in this case because of the generation of a strong coflow. Similarly placing the $\frac{1}{8}$ in. straight tube burner in the 1 in. diameter, tapered shroud (figure 26*c*) stabilized the flame, and increased the critical flow rate by more than 300%! One can only assume that the very different effects of the 2 and 1 in. shrouds were due to changes in flame shape and the relative changes in the magnitude of the co- and counterflows, and the details of the velocity profiles, in the two cases. Unfortunately, these latter quantities could not be measured during the present experiments. Similar effects have been noted by Cetegen & Ahmed (1993) in large diameter fires and plumes.

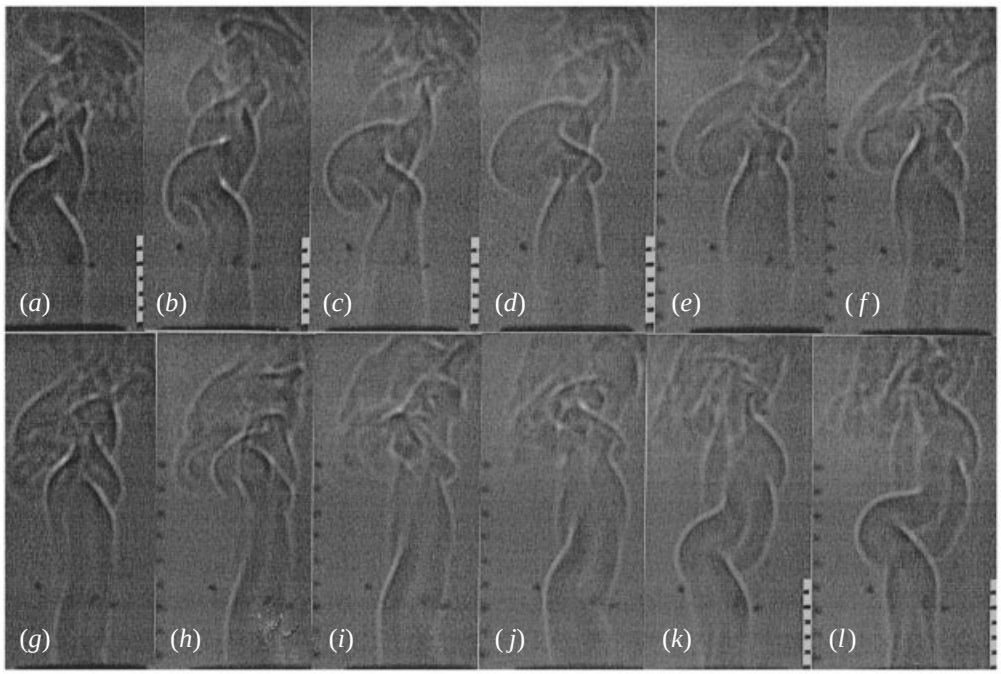

FIGURE 21. Time sequence of images of the helical flame/plume wandering found when a counterflow was applied to a stable flame.

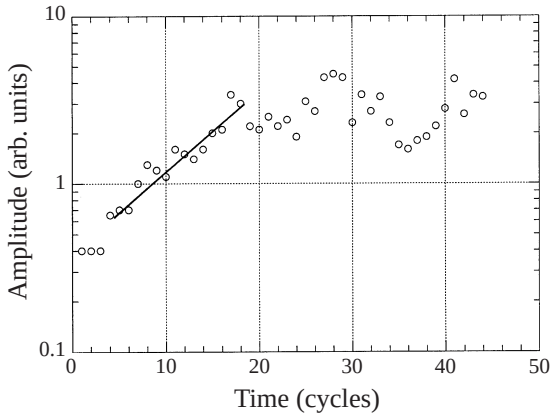

FIGURE 22. Growth of the flame amplitude shown in figure 20.

4. Conclusions and discussion

In the Sections above we have presented a number of results, both quantitative and qualitative, that can be interpreted in terms of the known facts concerning convective/absolute/global instabilities. The review article by Huerre & Monkewitz (1990) is probably the most useful reference in this regard. As is well known by now the transition from a convectively unstable state, where ambient disturbances are spatially amplified and swept downstream, to an absolute one, where disturbances grow spontaneously and can propagate up- and downstream and contaminate the whole flow, can be accomplished in a number of ways. The most clear-cut case where

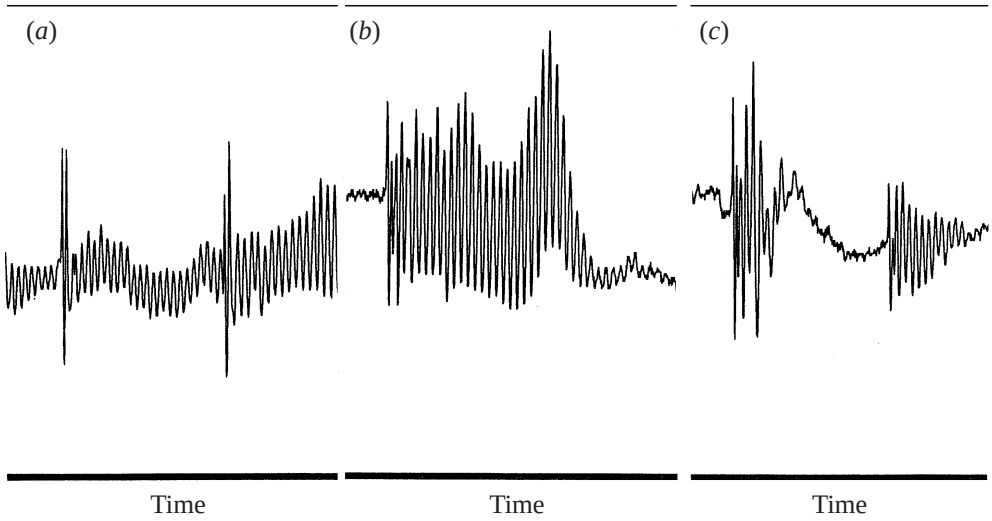

FIGURE 23. Flame amplitude as a function of time for the $\frac{1}{8}$ in. candle. (*a*) Flow rate of 42.9 ml min^{-1}, i.e. fully in the unstable regime. (*b*) 34.3 ml min^{-1}; this case is in the intermittent regime nearer the fully unstable situation. (*c*) 29.4 ml min^{-1}; also in the intermittent regime but close to the stable boundary.

an upstream propagation occurs is when a velocity profile containing a region of sufficiently strong back- or counterflow exists, e.g. the wake behind a cylinder at Reynolds numbers above 40. In some cases, e.g. the dripping faucet of Monkewitz *et al.* (1988), Le Dizes (1997), instability waves can propagate wave energy upstream and thus excite the whole flow, without any counterflow. In fact, one can think of the present problem as an inverted version of the dripping faucet, but with a different feedback mechanism.

For the present experiments the most relevant effect concerns the transition that occurs when either a wake is cooled or a jet is heated (HM, pp. 505–512). In this case, if a jet of given characteristics, i.e. Reynolds number, is heated it has been found to become locally absolutely unstable when the density ratio between jet and surroundings is less than approximately 0.66 (HM; also Monkewitz *et al.* 1990). When a sufficient length of jet has reached this state a global oscillation can be excited. The present case is, unfortunately, less clear-cut. The controlling parameter here is the fuel flow rate, while the velocity is produced by the buoyancy of the plume and not by an external mechanical source. Both the flow and the temperature fields are changed as this flow rate changes, so that one cannot simply vary one independently of the other as one can in the cases discussed in HM. For the candle flames, at low flow rates, the velocity at the base of the flame is essentially zero and the temperature is high; it is hypothesised that this flow is absolutely unstable. Higher in the flame/plume the velocity becomes large enough for the flow to be convectively unstable, in this case to a helical mode. As the flow rate is increased the region of absolutely unstable flow, close to the flame base, becomes longer and the origin of the convectively unstable region moves downward and closer to the location of the transition between the two states. At a critical flow rate it appears that the perturbations caused by the helical waves can propagate upstream, i.e. downwards, to help energize the instability. The region near the flame base then acts as a source of fluctuation energy for the whole plume.

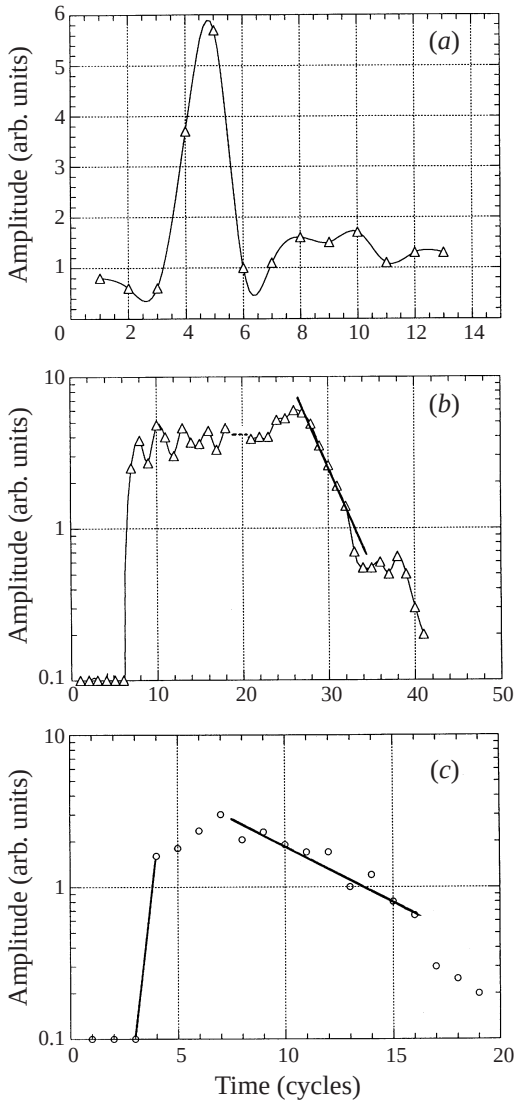

FIGURE 24. Amplitude versus time in cycles for the three cases shown in figure 23.

As mentioned above, this is essentially the scenario hypothesized by Monkewitz *et al.* (1988) for the case of the dripping faucet. In that case the flow has been shown to be absolutely unstable when the Weber number ($We = \sigma/\rho U^2 r$) is greater than 0.32. Here σ is the surface tension, U the jet velocity, r its radius and ρ its density. Monkewitz *et al.* (1988) found that the jet formed drops at a well-defined frequency when We exceeded 0.5 at a Reynolds number of 180, where the parameters were defined using values at the orifice. Here, at high flow rates, the convectively unstable jet formed drops far downstream; however, this formation of drops moved closer to the source as the flow rate was decreased. Eventually a transition to dripping took place when the convectively unstable flow had moved close enough to the orifice and the region of absolute instability had become large enough. The mathematical treatment of this type of problem has recently been presented by Chomaz, Huerre &

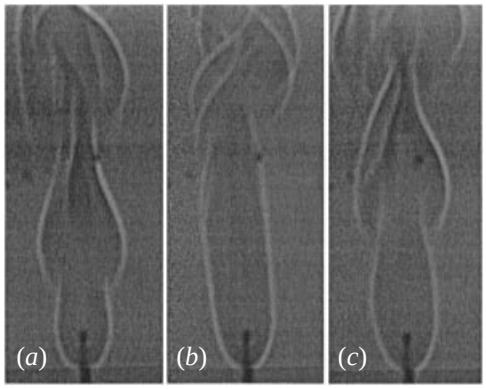

FIGURE 25. Images of the flame/plume for three conditions at 55.1 ml min^{-1} and the $\frac{1}{8}$ in. candle. (*a*) Unstable, flickering flame with the exit hole fully open. (*b*) Stabilized flame 15 s after a 15 cm high chimney was placed on the exit hole. (*c*) Re-established unstable flame 15 s after the chimney was removed.

Redekopp (1988; 1991), Monkewitz, Huerre & Chomaz (1993) and Le Dizes (1997) with general agreement as to mechanism but some disagreement as to the scaling properties of the flow. However the global nature of the instability was confirmed.

Alternatively one might postulate that there is a pressure feedback from some downstream flow interaction that generates a global response. This possibility, while it cannot be definitely rejected, seems to be at variance with observations of the insensitivity of the frequency of oscillation to details of the exit geometry.

In our case, following the heated jet example, the dimensionless control parameters are probably a Reynolds number $[g'R]^{1/2}R/\nu_P$ and a density ratio ρ_P/ρ_A, where ρ_P and ρ_A are the plume and ambient densities respectively, $g' = g[\rho_A - \rho_P]/\rho_P$ and R is a characteristic length, e.g. the burner radius. Of course it must also be noted that critical values of these quantities will only hold for a particular burner geometry and will most likely vary as burner characteristics are changed. This because the velocity field in the neighbourhood of the flame, and hence any co- or counterflow that tends to modify the plume stability, will be affected by these changes. Also, the values of ρ_P are the result of complex combustion processes and cannot be accurately specified, especially since not all the fuel is burned. Clearly the use of electrical heaters of high power density (0.5–1 kW cm^{-3}, in order to cover the same density range used in the flame experiments), the combustion of a pre-mixed flame for which the properties are better known, or helium/air mixtures would help alleviate this problem and allow a better determination of the correct parametric dependences of these systems at the high temperatures typical of the present experiments.

Using measured velocity profiles and calculated temperature profiles Lingens *et al.* (1996*b*) have shown that the profiles within the flame region are absolutely unstable under some circumstances. However they assume that the global oscillation is determined by the stability properties at one location, at the convective/absolute boundary, rather than by a finite region as proposed by HM. In practice the differences between the final states calculated from each are probably small but it is of some academic interest to choose the flow characteristics more precisely.

Also of interest is the fact that in the present case the density ratio between the flame/plume and its surroundings is very small, of order 0.2 to 0.15. This value is very much smaller than the smallest value found in most parallel-flow theoretical models of heated jets (e.g. the vortex sheet model of HM). This suggests that either

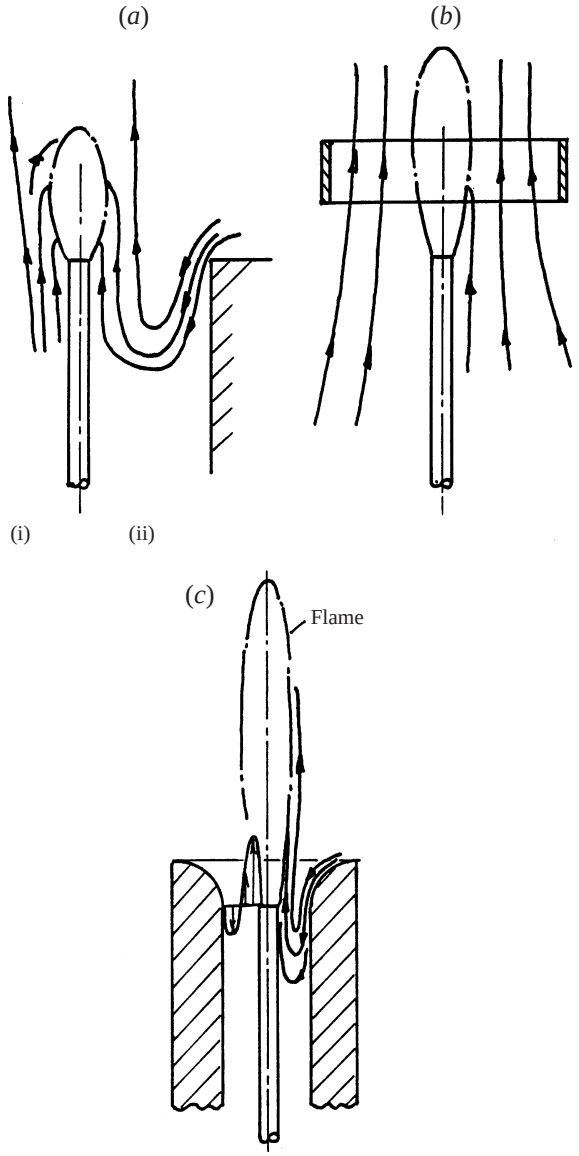

FIGURE 26. (*a*). Sketch of the streamlines induced by the flame when (i) flame was burning in free space, (ii) when it was surrounded by the 2 in. diameter tube (shroud). (*b*) Streamlines induced by a small shroud slightly above the burner lip. (*c*) Streamlines produced by the flame inside the smaller, 1 in. diameter, tapered shroud.

the flame/plume induces a large cold stabilizing coflow, and so needs a much smaller density ratio to become absolutely unstable, and/or the global structure of the very rapidly accelerating mean flow† is also a crucial ingredient of a complete and correct explanation of the observed phenomena.

† Elementary calculations suggest that the effective acceleration of fluid particles in the plume is of the order of 5 to 6 times the acceleration due to gravity, since there is no added mass effect. This is consistent with the LDA measurements of the heated flow outside the central jet core by Lingen *et al.* (1996*a*, *b*) for which the acceleration can be estimated to be approximately 5 g at a density ratio about 0.17.

A number of the observations presented in § 3 are also consistent with the suggestion that a global instability has been excited in the experiments reported in § 3. Considering the simple model of HM one can see that co(counter) flow is stabilizing (destabilizing) with respect to the transition to instability of the absolute type. In all cases shown here this appears to be the case, with co (counter) flow suppressing (enhancing) the axisymmetric instability. Also, the fact that the mode is axisymmetric is consistent with the prediction of that model. However note that the theory does not include the effects of buoyancy, which could, possibly, change the conclusions reached here. The observation that the frequency of oscillation is very stable and does not vary with height, and that the whole flame/plume, from the lowest point upwards, takes part in the oscillation is also consistent with a global or feedback excitation. As discussed earlier the purely convective theories are forced to choose some height at which the instability starts to grow and at which to calculate the flickering frequency. In the experiments this height is zero and the frequency calculated at that height also zero.

Also, evidence coming from the response to external disturbances should be considered. For example the response to a pulse suggests that when an axisymmetric perturbation is forced at the burner its reaction is to generate an axisymmetric perturbation that lasts for some time if it is in the intermittent zone, i.e. if the absolutely unstable region is marginally long enough. In the fully unstable region the pulse has no effect and in the completely stable region the perturbations die out very rapidly since the absolutely unstable region is not long enough to support the global mode. This is to be compared with similar observations in the problem of the dripping faucet.

All of these observations are strongly suggestive that the dynamics arise from a linearly destabilized global mode with a selection mechanism for the frequency that is entirely 'internal'.

What is particularly interesting from the results of this and prior work is the apparent lack of sensitivity of the oscillation frequency to the details of the source structure. Thus the $\frac{1}{2}$ in. candle, with and without an extension, for which the length of the flame at transition is very small and the flow entirely plume-like, and $\frac{1}{2}$ in. burners with extensive flames, give frequencies of oscillation that are virtually identical even though the flow rates may be somewhat different. This suggests that the simplest non-Boussinesq heated-plume model probably contains sufficiently complex dynamics to describe the types of motion seen in most experimental studies. This possibility is reinforced by the observations of Yuan *et al.* (1994) who discovered oscillations in a helium jet of the type found in both the present paper and the extensive literature on the problem. (The need for a non-Boussinesq formulation is emphasized by the observation that the Boussinesq plume results in a constant centreline velocity (Gebhart *et al.* 1988, p. 147). Since the present observations show that the plume is accelerating rapidly the latter model is unlikely to be the appropriate one on which to base a stability calculation.)

Finally, the most revealing, and conclusive, way to study this problem is to look at the response to forced sinusoidal oscillations, e.g. a sound source. This series of experiments will be more complex than those presented up to now and is presently underway. Proper presentation will require a discussion that is too long to add to the present paper and will be submitted at a later date.

The experiments reported here were performed at USC and ESPCI. The apparatus was constructed by Mark Trojanowski at the former institution; his help is recognised with thanks. Professor L. G. Redekopp of USC provided essential guidance during

the formative stages of the work and suggested many improvements and clarifications to the final manuscript. The help, both physical and financial, and important technical input from Drs Philippe Petitjeans and Jose Eduardo Wesfreid at the ESPCI was crucial to any success this work might have, and is acknowledged with deep gratitude. This paper was written while visiting the EPF Lausanne where the help of Professor P. A. Monkewitz is acknowledged. Discussions with Professor P. Huerre of the Ecole Polytechnique were also most helpful in deciding the scope of the work. Finally, I would like to thank Professor John Buckmaster for discussions and for pointing me towards the numerical solutions of Katta *et al.* (1994, 1996).

REFERENCES

Buckmaster, J. & Peters, N. 1986 The infinite candle and its stability–a paradigm for flickering diffusion flames. *21st Symp.* (*Intl*) *on Combustion*, pp. 1829–1836. The Combustion Institute.

Cetegen, B. M. & Ahmed, T. A. 1993 Experiments on the periodic instability of buoyant plumes and pool fires. *Combust. Flame* **93**, 157–184.

Chen, L. D. & Roquemore, W. M. 1986 Visualisation of jet flames. *Combust. Flame* **66**, 81–86.

Chen, L. D., Seaba, J. P., Roquemore, W. M. & Goss, L. P. 1988 Buoyant Diffusion Flames. *22nd Symp.* (*Intl*) *on Combustion*, pp. 677–684. The Combustion Institute.

Chen, L. D., Vilimpoc, V., Goss, L. P., Davis, R. W., Moore, E. F. & Roquemore, W. M. 1992 Time evolution of a buoyant jet diffusion flame. *24th Symp.* (*Intl*) *on Combustion*, pp. 303–310. The Combustion Institute.

Chomaz, J.-M., Huerre, P. & Redekopp, L. G. 1988 Bifurcations to local and global modes in spatially-developing flows. *Phys. Rev. Lett.* **60**, 25–28.

Chomaz, J.-M. Huerre, P. & Redekopp, L. G. 1991 A frequency selection criterion in spatially-developing flows. *Stud. Appl. Maths* **84**, 25–28.

Durox, D., Yuan, T. & Villermaux, E. 1997 The effect of buoyancy on flickering in diffusion flames. *Combust Sci. Tech.* **124**, 1–18.

Gebhart, B., Jaluria, Y., Mahajan, R. L. & Sammakia, B. 1988 *Buoyancy-Induced Flows and Transport*. Hemisphere.

Hamins, A., Yang, J. C. & Kashiwagi, T. 1992 An experimental investigation of the pulsation frequency of flames, *24th Symp.* (*Intl*) *on Combustion*, pp. 1695–1702. The Combustion Institute.

Huerre, P. & Monkewitz, P. A. 1990 Local and global instabilities in spatially developing flows. *Ann. Rev. Fluid Mech.* **22**, 473–537. (referred to herein as HM).

Katta, V. R., Goss, L. P. & Roquemore, W. M. 1994 Simulation of vortical structures in a jet diffusion flame. *Intl J. Numer Meth. Heat Fluid Flow* **4**, 413–424.

Katta, V. R., Goss, L. P., Roquemore, W. M. & Chen, L.-D. 1996 Dynamics of propane jet diffusion flames. *Atlas of Visualisation III* (ed. The Visualisation Society of Japan). CRC Press.

Koch, W. 1985 Local instability characteristics and frequency determination of self-excited wake flows. *J. Sound. Vib.* **58**, 53–83.

Le Dizes, S. 1997 Global modes in falling capillary jets. *Eur. J. Mech.* B: *Fluids* **16**, 761–778.

Lingens, A., Neemann, K., Meyer, J. & Schreiber, M. 1996*a* Instability of diffusion flames *26th Symp.* (*Intl*) *on Combustion*, pp. 1053–1061. The Combustion Institute.

Lingens, A., Reeker, M. & Schreiber, M. 1996*b* Instability of buoyant diffusion flames. *Exps. Fluids* **20**, 241–248.

Monkewitz, P. A., Bechert, D. W., Barsikow, B. & Lehmann, B. 1990 Self-excited oscillations and mixing in a heated round jet. *J. Fluid Mech.* **213**, 611–639.

Monkewitz, P. A., Davis, J., Bojorquez, B. & Yu, M.-H. 1988 The break-up of a liquid jet at high Weber number. *Bull. Am. Phys. Soc.* **32**, 2051.

Monkewitz, P. A., Huerre, P. & Chomaz, J. M. 1993 Global linear stability analysis of weakly non-parallel shear flows. *J. Fluid Mech.* **251**, 1–20.

Pierrehumbert, R. T. 1986 Spatially amplifying modes of the Charney baroclinic-instability problem. *J. Fluid Mech.* **170**, 293–317.

Rayleigh Lord 1929 *The Theory of Sound*. Macmillan.

Schoenbuecher, A., Arnold, B., Banhardt, K., Bieller, V., Kasper, H., Kaufmann, M., Lucas,

R. & Schiess, N. 1986 Simultaneous observation of organised density structures and the visible field in pool fires. *21st Symp.* (*Intl*) *on Combustion*, pp. 83–92. The Combustion Institute.

Yuan, T. 1993 Study of the dynamic behaviour of buoyant jet diffusion flames, PhD Thesis, Université Pierre et Marie Curie, Paris VI.

Yuan, T., Durox, D. & Villermaux, E. 1994 An analogue study for flickering flames. *Exps. Fluids* **17**, 337–349.

Zukosky, E. E., Cetegen, B. M. & Kubota, T. 1984 Visible structure of buoyant diffusion flames. *20th Symp.* (*Intl*) *on Combustion*, pp. 361–366. The Combustion Institute.